Canadian Metallurgical Quarterly, Vol 44, No 3 pp 305-312, 2005

Published by Canadian Institute of Mining, Metallurgy and Petroleum

THERMAL ANALYSIS STUDY OF THE EFFECT OF THE COOLING RATE ON THE MICROSTRUCTURE AND SOLIDIFICATION PARAMETERS OF 319 ALUMINUM ALLOY

S.G. SHABESTARI and M. MALEKAN

Faculty of Materials and Metallurgical Engineering, Iran University of Science and Technology (IUST), Narmak, Tehran, Iran

(*Received in revised form February, 2005*)

Abstract — In the metal casting industry, an improvement of component quality depends mainly on better control over the production parameters. Thus, a thermal analysis cooling curve of the alloy is used for process control in the aluminum casting industry. In this research, the effect of seven different cooling rates on the microstructure and solidification parameters of the 319 aluminum alloy have been investigated by means of thermal analysis. In each case, the cooling curve and its first derivative curve have been plotted by using very accurate thermal analysis equipment. The effect of different cooling rates on solidification parameters such as nucleation temperature ($T_{N,\alpha}$), nucleation undercooling ($\Delta T_{N,\alpha}$), recalescence temperature ($T_{R,\alpha}$), solidification range (ΔT_s) and total solidification time (t_f) has been studied in the liquidus region. Microstructural evaluation has been carried out and DAS was measured in all solidification conditions.

Résumé — Dans l'industrie de coulage des métaux, une amélioration de la qualité d'une composante dépend principalement d'un meilleur contrôle des paramètres de production. Ainsi, une analyse thermique de la courbe de refroidissement de l'alliage est utilisé pour le contrôle de procédé dans l'industrie de coulage de l'aluminium. Dans cette recherche, on a utilisé l'analyse thermique pour étudier l'effet de sept différents taux de refroidissement sur la microstructure et sur les paramètres de solidification de l'alliage d'aluminium 319. Dans chaque cas, on a tracé la courbe de refroidissement ainsi que la courbe de sa première dérivée en utilisant de l'équipement très précis d'analyse thermique. On a étudié, dans la région du liquidus, l'effet de différents taux de refroidissement sur les paramètres de solidification comme la température de nucléation ($T_{N,\alpha}$), la surfusion de nucléation ($\Delta T_{N,\alpha}$), la température de recalescence ($T_{R,\alpha}$) l'étendue de la solidification (ΔT_s) et la durée totale de solidification (t_f). On a effectué une évaluation de la microstructure et l'on a mesuré DAS sous toutes les conditions de solidification.

INTRODUCTION

The 319 (Al-Si-Cu) aluminum alloy has been widely used in the automotive industry due to its good casting characteristics and mechanical properties. In designing cast automotive parts, it is important to have an intimate knowledge of how the 319 alloy solidifies at different cross sections of the cast part and how this influences mechanical properties. This knowledge enables the designer to ensure that the casting will achieve the desired properties for its intended application.

A deeper understanding of the effect of the cooling rate on the solidification process has come to light in recent years [1-9]. The effect of the cooling rate on the structural features of 300 series alloys has been investigated by many authors [2-5,8,9]. According to their work, increasing the cooling rate refines all microstructural features including grain size, dendrite arm spacing (DAS) and intermetallic phases and improves silicon modification. It is well known that properties depend on the metallographic structures of metals, most noticeably secondary dendrite arm spacing (DAS). Also, DAS is affected by increasing the cooling rate much more than other microstructural features [4-8,10-14]. Radhakrishna and Seshan [5,6] concluded that DAS for three alloys is linearly related to solidification time, temperature gradient, freezing index and non-linearly to the ultimate tensile strength (UTS), yield strength (YS) and ductility. Hence, DAS has been used as a non-destructive and predictive indicator of properties. Furthermore, Jaquot and Hotz [7] found that microstructural

characteristics measured by an image analyzer could be used along with production parameters (356 composition, strontium modification, solidification conditions and metal quality) to predict mechanical properties. Flemings [8,15] had concluded that chilling improved not only soundness, but also, more importantly, affected the refinement in dendrite structure. He presented a generalized equation for secondary dendrite arm spacing for a wide variety of alloys (some aluminum, carbon steels and Fe-Ni alloys).

$$\text{DAS} = A(t_f)^c \quad (1)$$

or

$$\text{DAS} = B(C.R)^{-c} \quad (2)$$

where A and B are constants and C is in the range of 1/5 to 1/2. Much research has been focussed on the effect of the cooling rate on microstructural features and mechanical properties. However, changes in phase nucleation temperatures, nucleation and recalescence undercooling and solidification ranges with increasing cooling rates have not been extensively investigated in the literature.

Thermal analysis (TA) techniques monitor the temperature changes in a sample as it cools through a phase transformation interval. The temperature changes in the material are recorded as a function of the heating or cooling time in such a manner that allows for the detection of phase transformations. In order to increase accuracy, characteristic points on the cooling curve have been identified using the first derivative curve plotted versus time [16-19].

In the metal casting industry, an improvement of component quality depends mainly on better control over the production parameters. Thus, computer aided cooling curve thermal analysis (CA-CCTA) of alloys is used extensively for the evaluation of several processing and material parameters. Thermal analysis of alloys can provide information about the composition of the alloy, the latent heat of solidification, the evolution of the fraction solid, the types of phases that solidify and even dendrite coherency. There are also many other uses for TA such as determining dendrite arm spacing, degree of modification and grain refining in aluminum alloys, the liquidus and solidus temperatures, characteristic temperatures related to the eutectic regions and intermetallic phase formation [1-3, 17,18,20-25].

The microstructure developed during solidification depends not only on the nucleation and modification potential of the melt but also on the thermal gradient imposed during solidification by the mould. Thus, the microstructural features of the casting can be estimated by examining the characteristic parameters of the cooling curve obtained in a thermal analysis study. The effect of a grain refiner and a eutectic modifier on the microstructural features and the corresponding characteristic parameters of the cooling curve is usually evaluated for sand casting. If the thermal analysis technique is to be used for die casting, permanent mould casting or investment casting, then, the values of each characteristic thermal analysis parameter must be established to define the state of nucleation and the state of modification required in the melt for each of these casting processes [3].

The objectives of the present work are to study the effect of different cooling rates on the microstructural features and the characteristic parameters of the cooling curve of 319 aluminum alloy. Also, a numerical equation was proposed to predict cooling rates by measuring DAS in this alloy.

EXPERIMENTAL PROCEDURE

Commercial 319 aluminum alloy ingots were used in this study. The chemical composition is given in Table I. Ten kilograms of the alloy were melted in an electric resistance furnace and maintained at a temperature of 720 °C ± 5 °C. The melt was degassed for 10 minutes by rotary degassing equipment using argon inert gas. The melt was modified and the grain was refined by the addition of Al-10Sr and Al-5Ti-1B master alloys, respectively. The melt was maintained for 20 minutes after the addition of master alloys for complete dissolution. After melting, the oxide layer on the surface was skimmed and the molten metal poured into the moulds.

In order to achieve different cooling rates, seven moulds including CO_2 bonded silica sand with two different wall thicknesses, hot work tool steel (H13) with and without coating and thin wall steel with different coatings were used. All moulds were poured at two different conditions, first at room temperature and second preheated at 200 °C.

Cooling curve thermal analysis (CCTA) was performed on all samples using high sensitivity thermocouples of K type (Ni-Cr-Ni) that were protected in a stainless steel sheath and data were acquired by a high speed data acquisition system (A/D converter) linked to a notebook computer. Thermocouples were mounted on a test stand to avoid any vibration. The thermocouples were also located in the centre of the mould at a position of 25 mm from the bottom of the mould. In order to obtain reproducible results, the thermocouple was placed exactly at the same position for each experiment. All experiments were performed in a constant condition. The analog to digital (A/D) converter used in this work has a sensitive 16 bit converter (a resolution of $1/2^{16}$ or 0.0015%), response time of 0.02 seconds and a high accuracy of detection. The high end version of the thermal analysis pro-

Table I – Chemical composition of 319 aluminum alloy

Alloy composition	Elements							
	Si	Cu	Mg	Fe	Mn	Zn	Ti	Sr
319 (AA standard)	5.5-6.5	3-4	<0.1	<0.8	<0.5	<1	-	-
319 (Actual sample)	5.5	3.2	0.42	0.55	0.2	0.02	0.02	0.01

gram is a part of the thermal analysis system which simultaneously displays the cooling curves, first derivative curves and temperature and time on the monitor of the computer for an instant observation.

The cooling curve data was processed using a thermal analysis program and Excel software. The processing included smoothing, curve fitting, plotting the first derivatives, identifying the onset and end of solidification, determining solidification parameters such as cooling rate, nucleation temperature, nucleation undercooling, recalescence undercooling, solidification range and total solidification time.

Each chilled sample was sectioned horizontally where the tip of the thermocouple was located and it was prepared by standard grinding and polishing procedures. The final stage of polishing was done using commercial silicon oxide slurry. Optical microscopy was used to characterize the microstructure and intermetallic phases. Dendrite arm spacing (DAS) measurements were carried out using an image analyzer. The average of 30 DAS measurements was reported for each condition of the experiment. A numerical equation was proposed to predict cooling rates by measuring DAS. The effect of the cooling rate on the microstructure and solidification parameters was investigated in 319 aluminum alloy.
There are some differences in defining the thermal analysis parameters in the literature. To avoid this, the solidification parameters used in the present work are shown in Figure 1.

RESULTS AND DISCUSSION

The various parameters measured from cooling and derivative curves are the liquidus parameters, solidification range and total solidification time. As is evident from the cooling curve in Figure 1, there is a wide variation in the cooling rate during solidification. In this study, two types of cooling rates are calculated: in the first case, the cooling rate is calculated from the slope of the cooling curve above the liquidus region ($C.R_L$); in the second case, the cooling rate is computed from the slope of the straight line portion between the liquidus and eutectic regions (C.R). The cooling rates measured for the various experimental conditions ranged from 0.3 to 3 °C/s. This range covers the wide variety of cooling conditions which are used in the production of aluminum castings.

Cooling Curves

The cooling curves recorded for 319 alloy at various cooling rates are shown in Figure 2. It is seen that formation temperatures of the various phases are shifted when the cooling rate is increased. The shift magnitude increases with an increasing cooling rate. This shift changes the characteristic parameters of thermal analysis particularly in the liquidus region.

The arrows marked on the cooling curves in Figure 2 show three temperature arrest peaks that represent the various phase formation temperatures in the alloy system. The first peak shows the nucleation temperature of α aluminum primary phase, the second peak indicates Al+Si eutectic temperature and the third one shows the formation temperature of the Al_2Cu phase. Peaks corresponding to the formation of are not clearly visible at high cooling rates. In other words, as the cooling rate is increased, the cooling curves become less sharp.

The cooling rate is proportional to the heat extraction from the sample during solidification. Therefore, at a low cooling rate (0.52 °C/s), the rate of heat extraction from the sample is slow and the slope of the cooling curve is small. So, it creates a wide cooling curve. But, at a high cooling rate (2.1 °C/s) the rate of heat extraction from the sample is fast, the slope of the cooling curve is steep and it makes a narrow cooling curve.

Liquidus Parameters

Figure 3 shows the effect of the cooling rate on the nucleation temperature (liquidus temperature) of 319 alloy. As the cool-

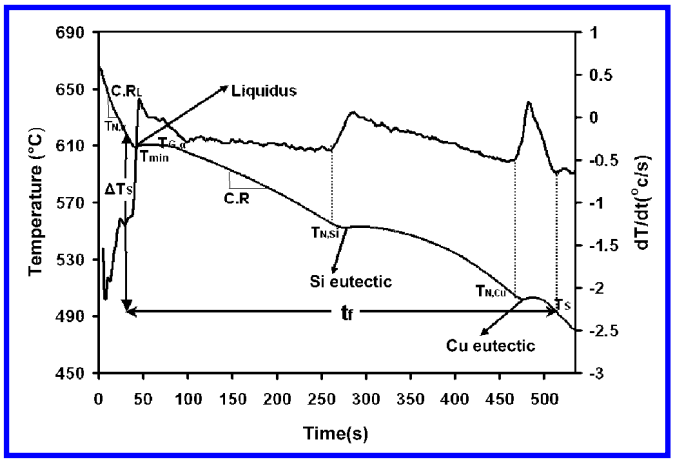

Fig. 1. Cooling curve, first derivative curve and representation of characteristic parameters used and analyzed in the present study for 319 alloy.

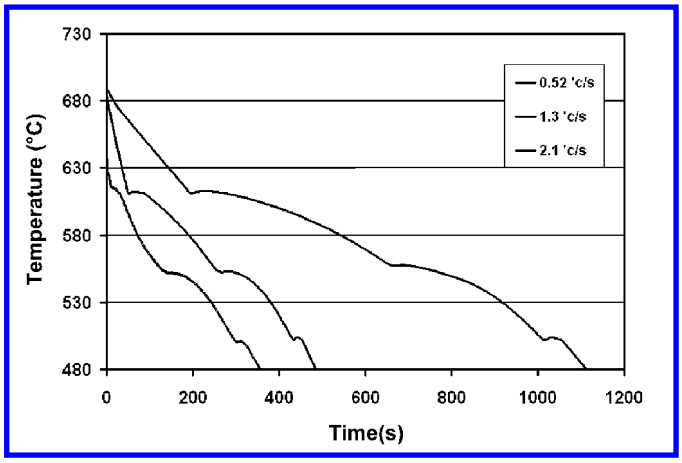

Fig. 2. Cooling curves of 319 alloy at various solidification conditions.

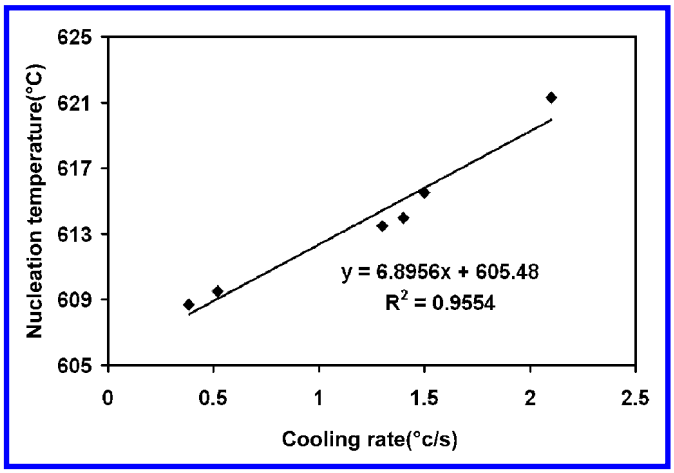

Fig. 3. Effect of the cooling rate on the nucleation temperature.

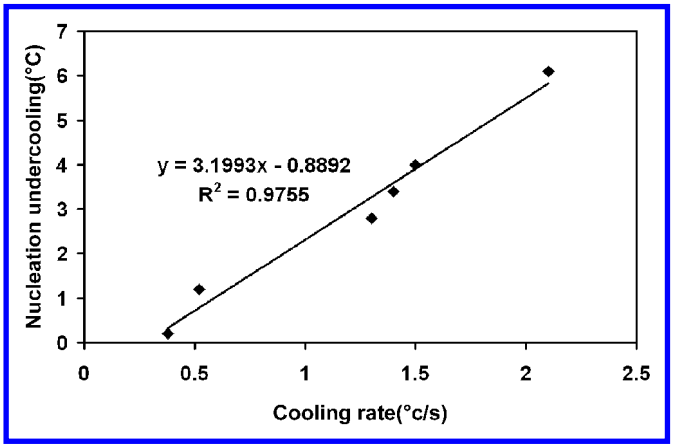

Fig. 4. Effect of the cooling rate on the nucleation undercooling temperature.

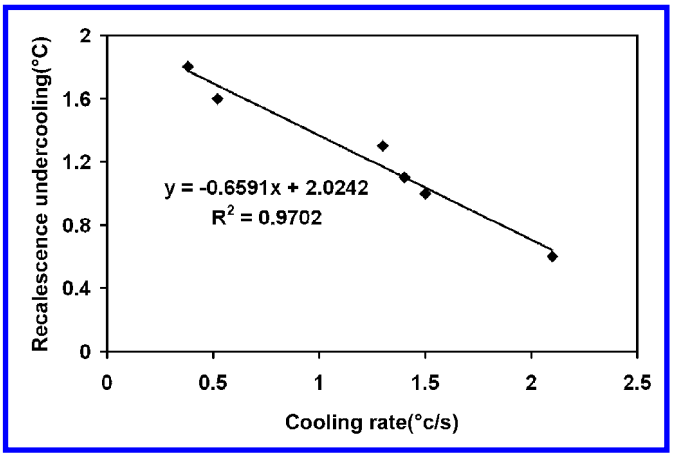

Fig. 5. Effect of the cooling rate on the recalescence undercooling temperature.

ing rate increases from 0.38 to 2.1 °C/s, the liquidus temperature increases from 608.7 to 621.3 °C. Increasing the cooling rate increases the heat extraction. Therefore, the melt is cooled to a lower temperature than the equilibrium melting point. This situation provides more nuclei to be nucleated because of the existing appropriate supercooling. Therefore, nucleation is continued easily and quickly.

The nucleation and recalescence undercooling temperatures, $\Delta T_{N,\alpha}$ and $\Delta T_{R,\alpha}$, measured for 319 alloy at various cooling rates are shown in Figures 4 and 5. The nucleation undercooling increases linearly with increasing cooling rate and the recalescence undercooling decreases linearly with increasing cooling rate. The increasing cooling rate from 0.38 to 2.1 °C/s increases the nucleation undercooling about 6 °C and the recalescence undercooling decreases from 1.8 to 0.6 °C.

A fast cooling rate increases the heat extraction rate from the melt and the existing nuclei in the melt become more activated. The growth condition is facilitated. Therefore, they will growth with a lower recalescence undercooling. The undercoolings, $\Delta T_{N,\alpha}$ and $\Delta T_{R,\alpha}$ in Figures 4 and 5 indicate the nucleation potential of the melt and can be used to control and predict the grain size of the castings.

Solidification Range and Total Solidification Time

The solidification range is defined as the difference in temperatures between the first and the last liquid to solidify. Total solidification time is also the time interval between the start and the end of solidification. Figures 6 and 7 show the effect of the cooling rate on the solidification range (ΔTs) and solidification time (t_f), respectively. As the cooling rate increases from 0.38 to 2.1 °C/s, the solidification range increases about 10 °C, but the total solidification time decreases about 580 seconds (about 9 minutes). It can also be seen in Figure 2 that a cooling curve obtained at the higher cooling rate has a shorter solidification time and larger solidification range. Solidification time is related to the cooling rate according to the equation [14]

$$t_f = A(C.R)^{-n} \quad (3)$$

where A and n are constants of the equation.

The solidification ranges for the formation and growth of the α-Al dendrites, ($\Delta T_\alpha = T_{N,\alpha} - T_{N,Si}$), Al-Si eutectic($\Delta T_{Si} = T_{N,Si} - T_{N,Cu)\ and}$ Cu rich phase ($\Delta T_{Cu} = T_{N,Cu} - Ts$) have been plotted versus the cooling rate in Figure 8. It is seen that increasing the cooling rate increases the solidification range of α-Al dendrites formation considerably, but has no effect on ΔT_{Si} and ΔT_{Cu}. Therefore, at high cooling rates, a greater volume of α-Al dendrites forms. The effect of the cooling rate on the solidification time of α-Al dendrites (t_α), Al-Si eutectic (t_{Si}) and Cu rich phase (t_{Cu}), is shown in Figure 9. As seen, a considerable decrease in total solidification time has occurred in the dendrite network growth and the Al-Si eutectic formation and this decrease is more significant in t_α. Gowri [2] has also reported the decreasing of total solidification time as a function of the cooling rate for 356 and 359 alloys. Solidification range and total solidification time are important input parameters for any solidification modelling.

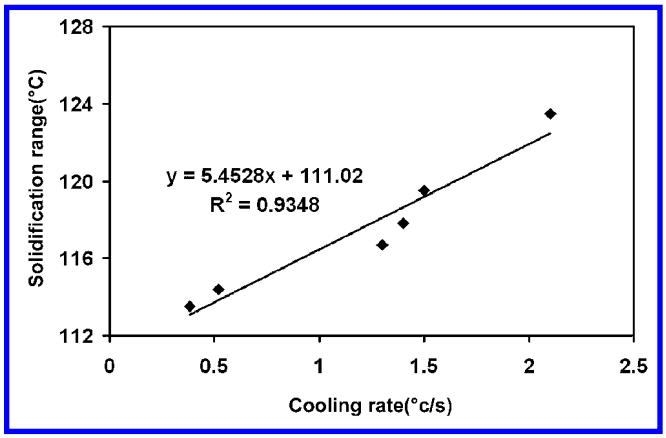

Fig. 6. Effect of the cooling rate on solidification range.

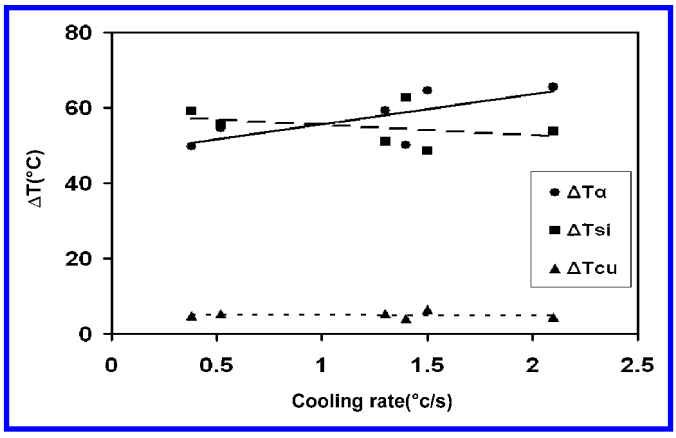

Fig. 8. Effect of the cooling rate on solidification range of various phases.

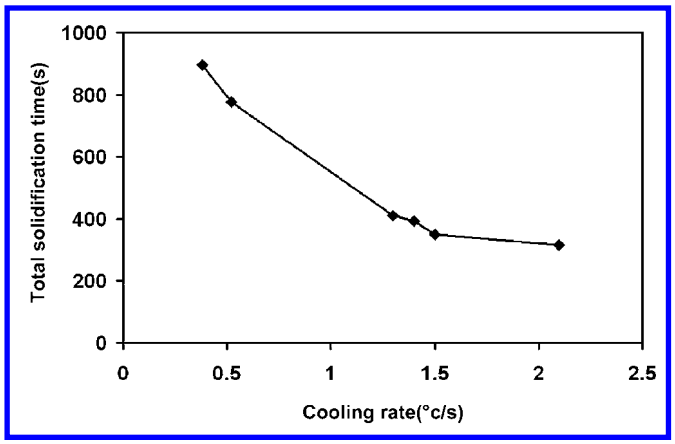

Fig. 7. Effect of the cooling rate on total solidification time.

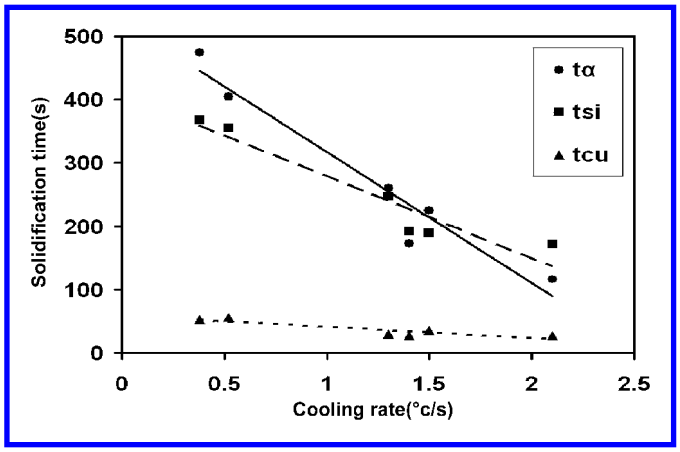

Fig. 9. Effect of the cooling rate on solidification time of various phases.

Dendrite Arm Spacing (DAS)

Figure 10 indicates the effect of the cooling rate on dendrite arm spacing of 319 aluminum alloy. As seen, increasing the cooling rate from 0.3 to 3 °C/s decreases the DAS about 60 per cent. Two reasons may be proposed for the changes of DAS as a function of the cooling rate:

1. Solid/liquid interface movement velocity increases with an increasing cooling rate and causes the increase of surface to volume ratio of dendrites. Therefore, it causes dendrite arm spacing to be reduced. In other words, where the solid/liquid interface movement velocity is high and because of the diffusion, more latent heat of melting can be released. So, thermal changes caused by the high cooling rate is dominant and the response of the system to this thermal situation is to reduce dendrite arm spacing and to increase the surface of dendrites.
2. Dendrite growth is slow at the high cooling rate because of the short solidification time and slow diffusion of atoms. Therefore, fine dendrites and reduced dendrite arm spacing are formed at the high cooling rates.

Figure 11 indicates the ln(DAS) as a function of ln(cooling rate). As shown in this Figure, the DAS varies linearly with the cooling rate in the logarithmic scale plot. The following relation between DAS and the cooling rate can be obtained by the least square method:

$$DAS = 46.758(C.R)^{-0.38} \quad (4)$$

where DAS is the dendrite arm spacing in micrometres and *C.R* is the cooling rate in degrees C/s. The coefficient of correlation and the standard deviation are 0.983 and 0.049, respectively. The DAS–C.R equation proposed for 319 alloy in this study is in a good agreement with what is reported by Flemings [8], Kurz and Fisher [16], Shivkumar and Apelian [10] and Caceres and Wang [12].

By measuring DAS using a simple metallography and Equation 4, the cooling rate can be determined in each section of an aluminum intricate shape and component such as an automobile cylinder head. Alloy chemical composition also influences the DAS, although the effect is lower than what is

obtained by the effect of the cooling rate. The specific DAS-C.R curve or equation is necessary for each alloy to be processed because the constants of Equation 2 are specific for each alloy.

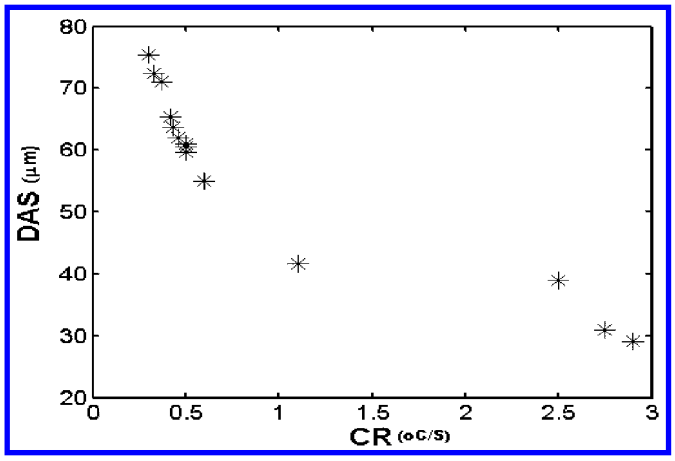

Fig. 10. Effect of the cooling rate on DAS in 319 alloy.

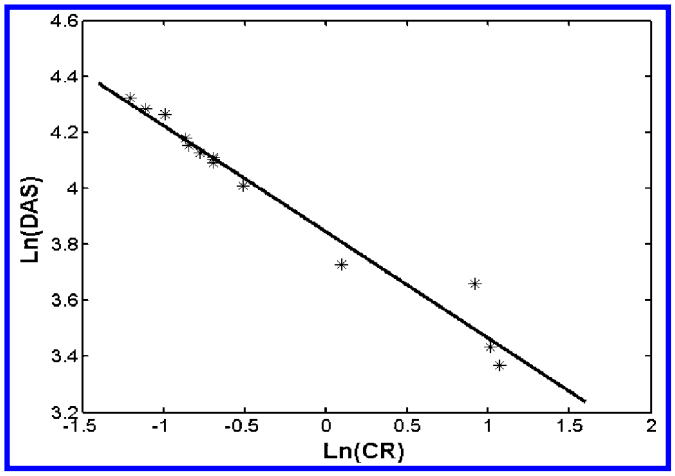

Fig. 11. The ln-ln plot of DAS as a function of the cooling rate.

Microstructure

The microstructures of some test samples of thermal analysis are shown in Figures 12 and 13. These two samples were solidified at cooling rates of 0.33 and 2.75 degrees C/s, respectively. The microstructures of the alloy include α- Al dendrites, eutectic silicon and intermetallic phases such as Al_5FeSi (β-phase), $Al_{15}(Fe,Mn)_3Si_2$ (α-phase) and Al_2Cu (Cu rich phase).

In the sample solidified at the high cooling rate, the DAS is fine (about 31 μm) and the Si structure indicates the effect of thermal modification (AFS modification rate = 4-5). In the sample solidified at a low cooling rate, the DAS is coarse (about 72 μm) and the Si modification rate is small

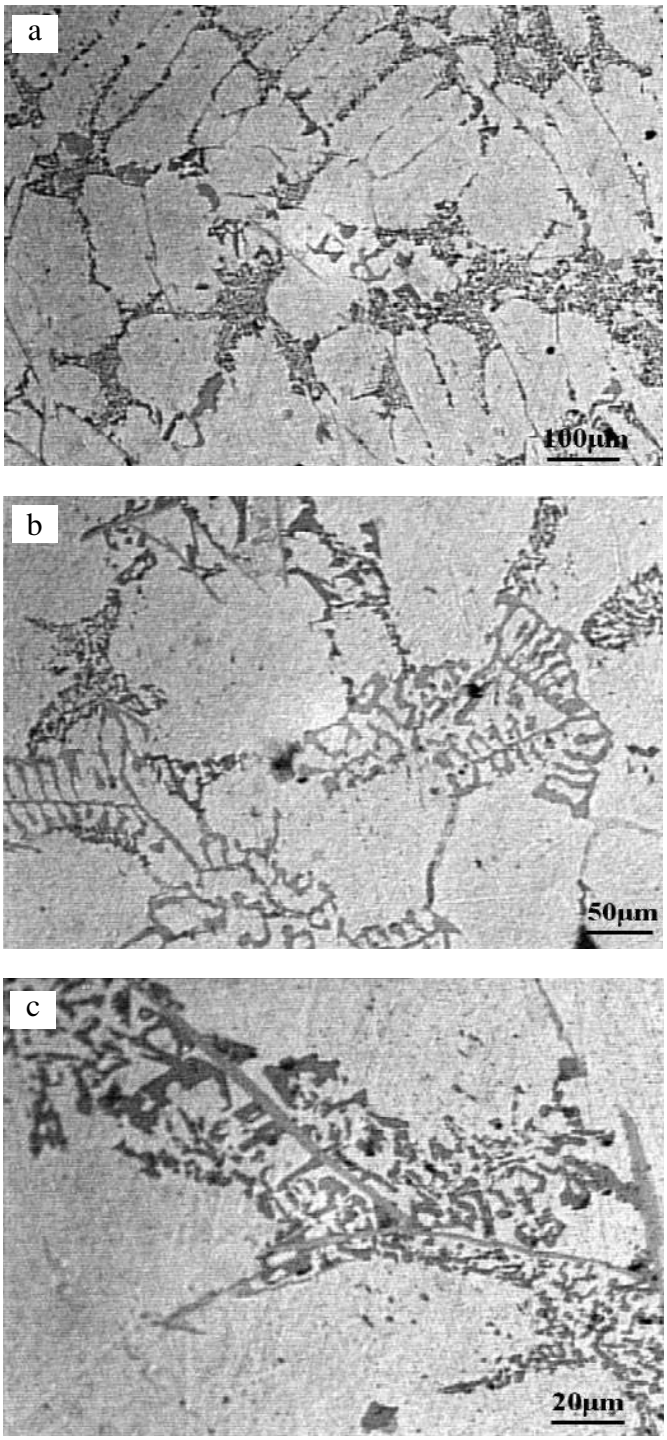

Fig. 12. Microstructure of 319 alloy solidified at the cooling rate of 0.33 °C/s a) 100×, b) 200× and c) 500×.

(about 2-3). Therefore, Figure 12c indicates the partially modified microstructure that occurs when 0.01 wt%Sr is added to the melt and the cooling rate is low (0.33 °C/s) and Figure 13c shows the full modified microstructure by the addition of the same amount of Sr when the cooling rate is

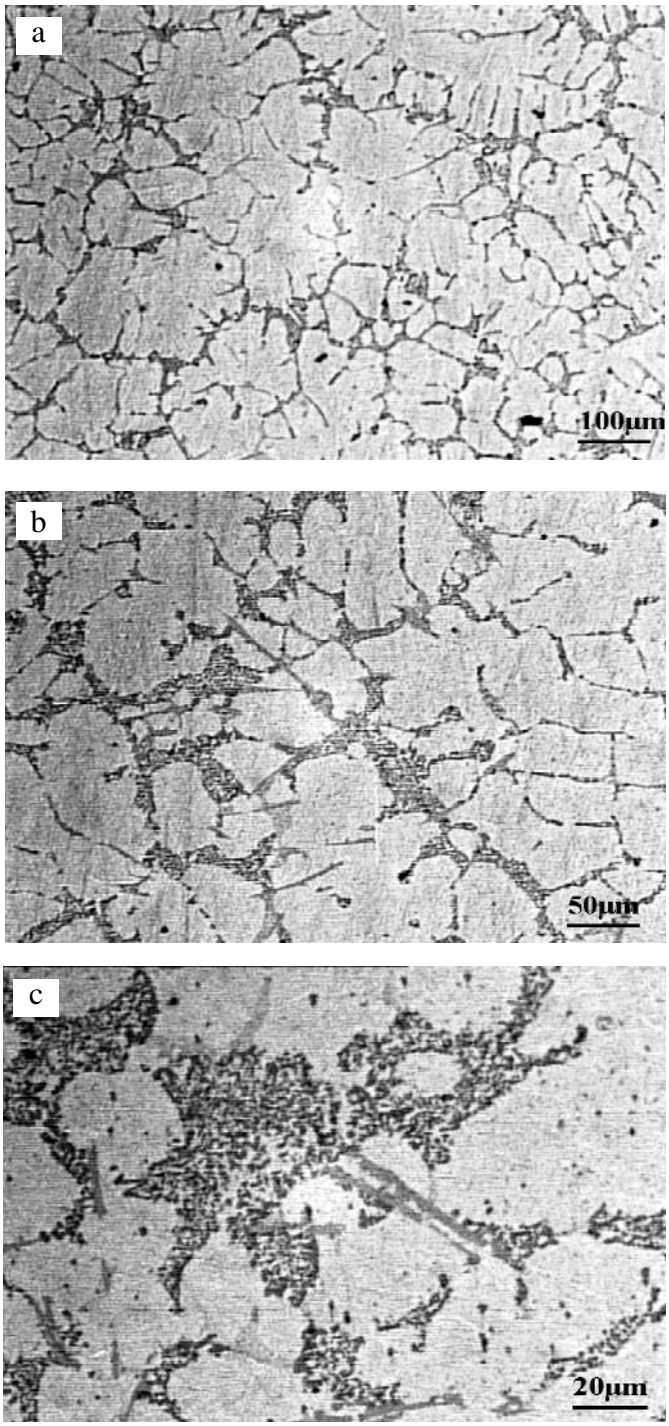

Fig. 13. Microstructure of 319 alloy solidified at the cooling rate of 2.75 °C/s a) 100×, b) 200× and c) 500×.

high (2.75 °C/s). Therefore, decreasing the cooling rate postpones the eutectic Si modification; however, the high cooling rate prevailing in the permanent mould casting and die casting requires much lower levels of modifier compared to sand casting processes. Thus, the cost and porosity problems can be minimized by avoiding the use of excess additions of silicon modifier.

Figure 13 also shows that at low cooling rates an $Al_{15}(Fe,Mn)_3Si_2$ phase is developed along with the dendritic growth of α-Al. The $Al_{15}(Fe,Mn)_3Si_2$ phase is revealed as Chinese script morphology. The needle phase of Al_5FeSi (β-phase) forms at the low cooling rate. However, α-Al and $Al_{15}(Fe,Mn)_3Si_2$ phases form in the interdendritic regions at higher cooling rates.

CONCLUSIONS

The effect of the cooling rate on the microstructural features such as DAS, eutectic silicon, intermetallic phases and thermal analysis characteristic parameters were studied. The results are summarized as follows:

1. Solidification parameters are affected by the cooling rate. The formation temperatures of various phases are shifted with an increasing cooling rate.

2. The plot of DAS as a function of the cooling rate shows a linear relationship in a logarithmic scale. Increasing the cooling rate from 0.3 to 3 °C/s decreases DAS about 60%. A numerical equation was proposed to predict cooling rates by measuring DAS in 319 aluminum alloy.

3. Increasing the cooling rate increases significantly the liquidus temperature, nucleation undercooling temperature, solidification range and decreases the recalescence undercooling temperature and total solidification time.

4. Increasing cooling rate refines all microstructural features including dendrite arm spacing (DAS) and intermetallic compounds and improves silicon modification.

ACKNOWLEDGEMENTS

The assistance of the staff of the Advanced Solidification Laboratory of the Iran University of Science and Technology (IUST) is acknowledged. Also, the authors would like to thank the technical support of Iran Khodro Vehicle Manufacturing Company, particularly, Mr. A. Sadian, head of the Iran Khodro Aluminum Casting Company.

REFERENCES

1. R.I. MacKay, M.B. Djurdjevic and J.H. Sokolowski, "Effect of Cooling Rate on Fraction Solid of Metallurgical Reactions in 319 Alloy", *AFS Transactions*, 2000, vol. 108, pp. 521-530.
2. S. Gowri, "Comparison of Thermal Analysis Parameters of 356 and 359 Alloy", *AFS Transactions*, 1994, vol. 102, pp. 503-508.
3. L. Ananthanarayanan, F.H. Samuel and J. Gruzleski, "The Thermal Analysis Studies on the Effect of Cooling Rate on the Microstructure of the 319 Aluminum Alloy", *AFS Transactions*, 1992, vol. 100, pp. 383-391.

4. H. Matuja, B.C. Giessen and N.J. Grant, "The Effect of Cooling Rate on the Dendrite Spacing in Splat-Cooled Aluminum Alloys", *The Journals of the Institute of Metals*, 1968, vol. 9, pp. 30-32.
5. K. Radhakrishna, S. Seshan and M.R. Seshadri, "Dendrite Arm Spacing in Aluminum Alloy Casting", *AFS Transactions*, 1980, vol. 88, pp. 695-701.
6. K. Radhakrishna and S. Seshan, "Dendrite Arm Spacing and Mechanical Properties of Aluminum Alloy Casting", *Cast Metals*, 1989,vol. 2(1), pp. 34-38.
7. J.C. Jaquet and W. Hotz,"Quantitative Description of the Microstructure of Aluminum Foundry Alloys", *Cast Metals*, 1992, vol. 4(4), pp. 200-225.
8. M.C. Flemings, T.Z. Kattamis and B.P. Bardes, "Dendrite Arm Spacing in Aluminum Alloys", *AFS Transactions*, 1991, vol. 99, pp. 501-506.
9. A.M. Figueredo, Y. Sumartha and M.C. Flemings, "Measurement and Calculation of Solid Fraction in Quenched Semi-Solid Melts of Rheocast Aluminum Alloy A357", *Light Metals*, 1998, B. Welch, ed.,The Minerals, Metals and Materials Society, pp. 1103-1106.
10. S. Shivkumar, L. Wang and D. Apelian, "An Overview on Molten Metal Processing of Advanced Cast Aluminum Alloys", *JOM*, 1991, pp. 26-32.
11. G.F. Salas, M.E. Noguez, J.G. Ramirez and T. Robert, "Application of Secondary Dendrite Arm Spacing-Cooling Rate Equation for Cast Alloys", *AFS Transactions*, 2000, vol. 108, pp. 593-597.
12. C.H.Caceres and Q.G. Wang, "Dendrite Cell Size and Ductility of Al-Si-Mg Casting Alloys: Spear and Gardner Revisited", *Int. J. Cast Metals Res*., 1996, vol. 9, pp. 157-162.
13. P.N. Crepeau, W.T. Whited and M.E. Hoover, "Automatic Assessment of Dendrite Cell Spacing in Cast Aluminum Microstructures", *AFS Transactions*, 1997, vol. 105, pp. 775-781.
14. P. Kumar and J.L. Gaindhar, "DAS, Solidification Time and Mechanical Properties of Al-11%Si Alloys V-Processed Castings", *AFS Transactions*, 1997, vol. 105, pp. 635-638.
15. M.C. Flemings, *Solidification Processing*, 1974, Mc Graw-Hill, New York.
16. W. Kurz and D.J. Fisher, *Fundamentals of Solidification*, 1998, Switzerland, Trans. Tech. Publication, Rockport, MA.
17. L. Backuerud, G. Chai and J. Tamminen, *Solidification Characteristics of Aluminum Alloys*, 1990, vol. 2: Foundry Alloys, AFS/ Skanaluminium, Stockholm, Sweden.
18. J. Tamminen, *Thermal Analysis for Investigation of Solidification Mechanisms in Metals and Alloys*, 1988, PhD. thesis published in *Chemical Communications*, University of Stockholm, Sweden, No. 2.
19. T. Hatakeyama and Liu Zhenhai, *Handbook of Thermal Analysis*, 1998, John Wiley and Sons Ltd, England, pp. 3-6.
20. A.M. Samuel, P. Ouellet, F.H. Samuel and H.W. Doty, "Microstructural Interpretation of Thermal Analysis of Commercial 319 Al Alloy With Mg and Sr Additions", *AFS Transactions*, 1997, vol. 105, pp. 951-962.
21. J.O. Barlow and D.M. Stefanescu, "Computer-Aided Cooling Curve Analysis Revisited," *AFS Transactions*, 1997, vol. 105, pp. 349-354.
22. R.I. Mackay, M.B. Djurdjevic, H. Jiang, J.H. Sokolwski and W.J. Evans, "Determination of Eutectic Si Particle Modification Via a New Thermal Analysis Interpretive Method in 319 Alloy", *AFS Transactions*, 2000, vol. 108, pp. 511-520.
23. D. Emadi and L.V. Whiting, "Determination of Solidification Characteristics of Al-Si Alloys by Thermal Analysis", *AFS Transactions*, 2002, vol. 200(033).
24. M.B. Djurdjevic, W.T. Kierkus, G.E. Byczynski, T.J. Stockwell and J.H. Sokolowski, "Modeling of Fraction Solid for 319 Aluminum Alloy", *AFS Transactions*, 1999, vol. 107, pp. 173-179.
25. M.B. Djurdjevic, W.T. Kierkus, R.E. Liliac and J.H. Sokolowski, "Extended Analysis of Cooling Curves," *41th Annual Conference of Metallurgists of CIM 2002, Proceedings of the International Symposium on Light Metals*, 2002, pp. 351-365.